Dependence of spectroscopic properties on doping content and temperature of bismuth-doped lanthanum aluminosilicate glass

Min Qian (钱 敏)[1,2*], Jimeng Cheng (程继萌)[1], and Lili Hu (胡丽丽)[1]

[1]*Key Laboratory of Materials for High Power Laser, Shanghai Institute of Optics and Fine Mechanics, Chinese Academy of Sciences, Shanghai 201800, China*

[2]*Graduate University of Chinese Academy of Sciences, Beijing 100049, China*

[*]*Corresponding author: qianminjstz@126.com*

Received April 14, 2012; accepted May 17, 2012; posted online September 28, 2012

The effects of bismuth doping content and temperature on the absorption property and near-infrared (NIR) luminescence of Bi-doped La_2O_3-Al_2O_3-SiO_2 (LAS) glasses are presented. The emission intensity reaches the maximum when the Bi_2O_3 content in 3.0Bi-LAS is 1.83%. The emission spectra reach their peaks at 1 190 and 1 117 nm, with full-width at half-maximum (FWHM) values of 330 and 228 nm under 500 and 700-nm excitations, respectively. As the Bi_2O_3 content increases, the peak wavelengths and FWHMs of emission bands increase, but their lifetimes decrease. The lifetime of 2.0Bi-LAS is 460 μs at 9 K, and is almost temperature independent until 350 K. The NIR emission of Bi in the system has strong resistance to thermal quenching from 9 to 350 K.

OCIS codes: 160.0160, 160.2750, 070.4790.

doi: 10.3788/COL201210.111602.

Bismuth-doped glasses have attracted considerable attention as materials for broadband amplifiers and tunable lasers that cover all telecommunication wavelengths from 1 100 to 1 600 nm since ultra-broadband, near-infrared (NIR) fluorescence and the relevant optical amplification have been reported by Fujimoto *et al.*[1,2]. The spectroscopic properties of Bi-doped glasses have been widely investigated in various glass hosts, such as silicate[3−9], phosphate[10,11], germanate[12−15], bismuthate[16], and chalcogenide glasses[17,18]. The full-width at half-maximum (FWHM) of the NIR luminescence band was reported to reach up to 600 nm in a Bi-doped chalcogenide glass. The FWHM can even reach 850 nm at cryogenic temperature[17], and the decay time of NIR emission reaches up to 1 725 μs in a Bi-doped aluminogemanate glass[15].

Compared with other glass hosts, silicate glasses are more remarkable in terms of compatibility with commercial silica fiber networks. Alkali or alkaline earth oxides are commonly used in silicate glass hosts as network modifiers, but they increase the optical basicity of glasses, which is reported to be harmful to NIR emissions of Bi-doped glasses[8]. Compared with the M-O bond-strengths of alkali- and alkali earth-based glasses, La-O bonds are stronger, because of the high field-strength of La^{3+} ions. Lanthanum aluminosilicate (LAS) glasses exhibit high glass transition temperatures that range from 800 to 900 °C and are virtually independent of the composition[19]. Excellent physical properties and lower optical basicity make LAS glasses potential hosts for bismuth doping.

To our knowledge, no research on Bi-doped LAS (La_2O_3-Al_2O_3-SiO_2) system glasses has been performed. In this letter, we select the composition of $65SiO_2$-$20Al_2O_3$-$15La_2O_3$ (in mole%) as the host of bismuth doping. The composition has been chosen based on the glass forming region in a previous work[20]. The influence of Bi_2O_3 content and temperature on the spectroscopic properties of bismuth ions in La_2O_3-Al_2O_3-SiO_2 glass is also investigated.

The analytical-grade reagents of SiO_2, $Al(OH)_3$, La_2O_3, and Bi_2O_3 were used as starting materials. Glass compositions (in mol%) of $65SiO_2$-$20Al_2O_3$-(15-x)La_2O_3- xBi_2O_3 (x = 0.5, 1.0, 2.0, 3.0, and 4.0 mol%) were studied and named as xBi-LAS, where x = 0.5 to 4.0 mol%. The mixed 40-g batches were melted in silica ceramic crucibles at 1 600 °C at room temperature for 3 h. The glass melt was poured on the pre-heated steel mold and annealed at 700 °C for 200 min. The color of the glass samples changed from pink to brownish red as the of Bi_2O_3 doping level increased. Considering the volatilizing losses of bismuth during the melting process, the real bismuth content was measured using inductively coupled plasma atomic emission spectroscopy. Bi_2O_3 concentrations in 0.5, 1.0, 2.0, 3.0, and 4.0Bi-LAS were 0.40, 0.63, 1.28, 1.83 and 2.58 mol%, respectively.

The glasses were cut and polished to a 10×25×3-(mm) size for optical measurements. The optical absorption spectrum was measured by a Lambda spectrophotometer (900UV/VIS/NIR , Perkin-Elmer, USA). The fluorescence spectra and fluorescence decay were obtained using a steady state spectrometer (FLSP920, Edinburgh, England). A xenon lamp was used as the pumping source. Liquid helium was used to achieve low temperatures.

Figure 1 shows the absorption spectrum of 0.5Bi-LAS glass ranging from 300 to 1 600 nm with a sample thickness of 3 mm. The absorption spectrum consists of five peaks. Peaks at approximately 500 and 700 nm and a shoulder at 800 nm are similar, as reported in other bismuth-doped glasses[1,13]. An ultra-broad absorption band exists, ranging from 850 to 1 400 nm with an absorption peak at approximately 1 100 nm. A weak absorption band at approximately 1 420 nm can be observed in Fig. 1. This has also been observed in previous stud-

ies on Bi-doped fibers[21,22]. The absorption spectra are similar in glasses with different Bi_2O_3 doping levels.

The absorption cross sections σ_{abs} at 500 and 700 nm, which are the primary absorption bands of bismuth ions[1], are calculated using

$$\sigma_{abs} = \frac{2.303 \lg(I_0/I)}{NL}, \quad (1)$$

where I_0 is the initial incidence intensity, I is the transmitted intensity, N is the bismuth ion concentration, and L is the sample thickness. We used L=0.3 cm, and calculated N as $N = \frac{\rho\omega N_A}{M_{Bi_2O_3}}$, where ρ is the density of glass, ω is the mass percentage of Bi_2O_3, and $M_{Bi_2O_3}$ is the molar mass of Bi_2O_3. The σ_{abs} of the Bi-LAS samples reaches 8.31×10^{-21} cm^2 at 500 nm.

The inset of Fig. 1 shows the concentration dependences of the absorption cross sections (σ_{abs}) at 500 and 700 nm. The σ_{abs} increases as the Bi_2O_3 content increases. When the Bi_2O_3 content is less than 2 mol% (e.g., 3.0 Bi-LAS), the σ_{abs} at 500 nm and the content follow a linear trend. The slope of the line decreases as the Bi_2O_3 content increases. Moreover, σ_{abs} at 700 nm and the Bi_2O_3 content both increase as the slope decreases. This phenomenon occurs because less active bismuth centers form when the Bi_2O_3 doping level is larger than a certain limit.

Figures 2(a) and (b) show the emission spectra of bismuth-doped La_2O_3-Al_2O_3-SiO_2 glasses with various bismuth doping levels under the 500 and 700-nm excitations, respectively. These figures also show a substantial increase in NIR luminescent intensity with increasing Bi_2O_3 content up to 1.83 mol% in 3.0 Bi-LAS. The intensity reduction in high bismuth doping levels likely results from concentration quenching. In addition, the peak wavelengths and asymmetry of emission bands gradually increase as the Bi_2O_3 contents increase under the 500 and 700-nm excitations.

Figure 3 shows the FWHM and peak wavelength of the emission spectra as a function of Bi_2O_3 content. The red-shift of the emission peaks with increasing Bi_2O_3 content, as observed in Fig. 2, is visualized in Fig. 3. The FWHM also increases along with the increase in bismuth doping level (Fig. 3), even when the emission intensity decreases in 4.0Bi-LAS glass.

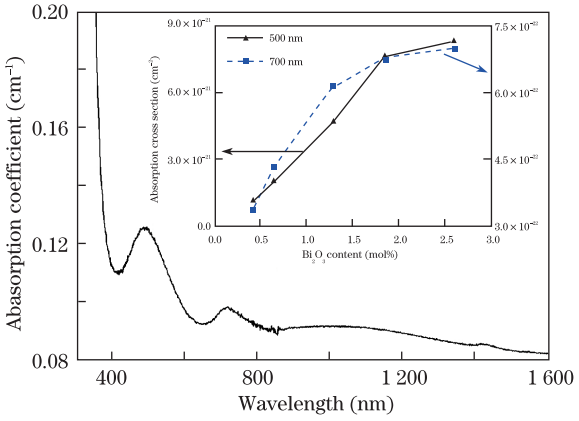

Fig. 1. Absorption spectrum of Bi-LAS glass with a sample thickness of 3 mm. The inset plots the absorption cross section as a function of Bi_2O_3 content.

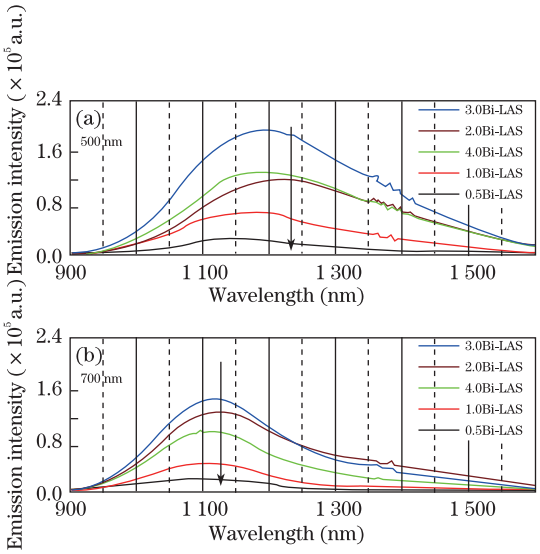

Fig. 2. Emission spectra of Bi-LAS glass samples with various bismuth doping levels under (a) 500- and (b) 700-nm excitations.

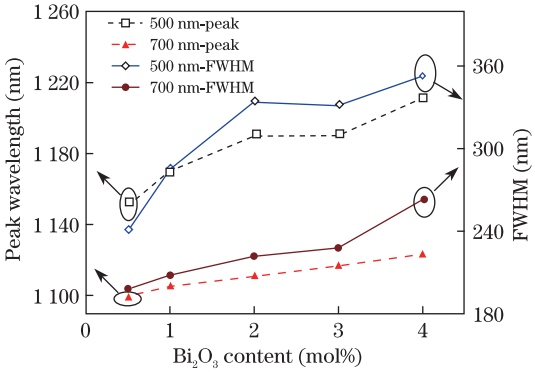

Fig. 3. Emission peak wavelengths and FWHM values as functions of Bi_2O_3 content.

To investigate the emission properties for high bismuth doping levels, the emission bands of 4.0Bi-LAS under the 500 and 700-nm excitations were deconvoluted to Gaussians, as shown in Figs. 4(a) and (b), respectively. The two emission bands are deconvoluted to 2 Gaussians with a determination coefficient $R^2 > 0.999$. The emission spectrum under the 500-nm excitation consists of two emission bands at 1 160 (peak 1) and 1 320 nm (peak 2). The emission spectrum excited at 700 nm is deconvoluted to 2 peaks positioned at 1 100 (peak 1) and 1 300 nm (peak 2). Similar Gaussian fitting results have been observed in other Bi-doped materials[5,23]. The emission spectra Gaussian fitting results of other Bi-LAS glass samples are roughly the same as those shown in Fig. 4. Table 1 shows the ratio of Gaussian peaks, which are calculated by dividing the integrated area of peak 2 with the integrated area of peak 1 in all Bi-LAS glasses. The ratios increased from 0.49 to 1.95 under the 500-nm excitation and from 0.37 to 1.22 under the 700-nm excitation as the Bi_2O_3 content increased from 0.40% to 2.58%. The different concentration dependencies of the Gaussian peaks cause the red-shifting and broadening of the emission bands in Fig 3. Similarly, the asymmetric

Table 1. Integrated Areas of Deconvoluted Gaussian Peaks under the 500- and 700-nm Excitations for Various Bi_2O_3 Contents

Bi_2O_3 Content (mol%)	500 nm-excitation Integrated Area Peak1 ($\times10^7$)	500 nm-excitation Integrated Area Peak2 ($\times10^7$)	Ratio	700 nm-excitation Integrated Area Peak1 ($\times10^7$)	700 nm-excitation Integrated Area Peak2 ($\times10^7$)	Ratio
0.5	0.43	0.21	0.49	0.36	0.13	0.37
1	1.03	0.96	0.93	0.78	0.31	0.40
2	1.68	2.65	1.58	1.40	0.85	0.60
3	2.53	4.00	1.58	2.05	1.58	0.77
4	1.39	2.71	1.95	1.54	1.88	1.22

emission bands at higher bismuth doping levels resulted from the increased contribution of peak 2 to the emission band. Furthermore, the different concentration dependence indicates that two emission centers may exist. One is responsible for the emission band at around 1 100 nm and the other is responsible for the emission band at 1 300 nm[23]. The different locations of the emission bands under various exciting wavelengths can be ascribed to the different proportions of the emission peaks.

We used X-ray photoelectron spectroscopy (XPS) to explore the valence states of active Bi ions in Bi-LAS glasses. Figures 5(a–c) show the XPS peaks of Bi($4f_{5/2}$, $4f_{7/2}$) on 1.0 and 2.0Bi-LAS glasses and Bi_2O_3 powders, respectively. The red dashed curves of Figs. 5(a) and (b) indicate the Bi($4f_{5/2}$, $4f_{7/2}$) peaks, and are the fitting curves of the measured results. The main Bi($4f_{5/2}$, $4f_{7/2}$) peaks of both 1.0 and 2.0Bi-LAS glasses are at 163.8 and 158.5 eV, respectively. No significant shifts are observed in the XPS spectra of 1.0 and 2.0Bi-LAS glasses. Therefore, the Bi_2O_3 doping level does not affect the valence state of Bi ions in Bi-LAS glasses. Compared with the XPS spectrum of Bi_2O_3 powders in Fig. 5(c), the Bi($4f_{5/2}$, $4f_{7/2}$) peaks of Bi-LAS glasses in Figs. 5(a) and (b), which are 164.1 and 158.8 eV respectively, shift to a lower energy at 0.3 eV. The energy shift proves the existence of Bi ions with valence states lower than +3

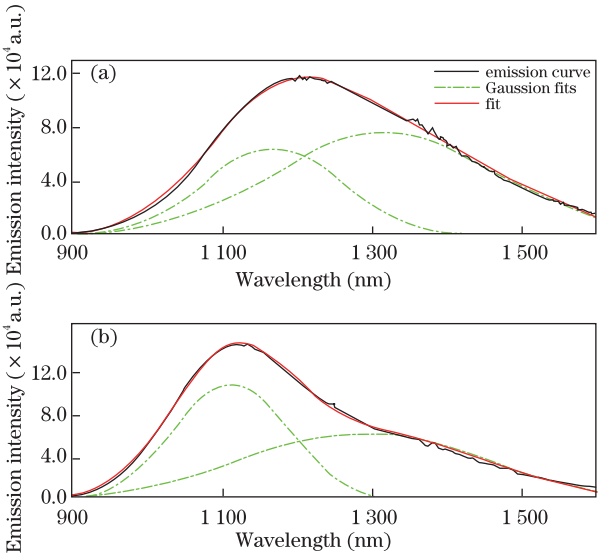

Fig. 4. Emission spectra deconvoluted into Gaussians of 4.0Bi-LAS glass excited at (a) 500 and (b) 700 nm.

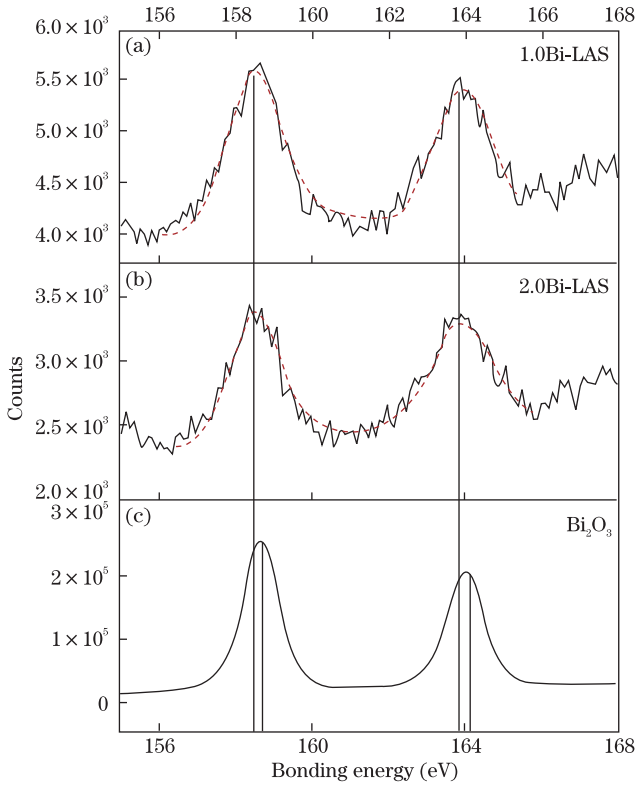

Fig. 5. X-ray photoelectron spectroscopy peaks of Bi($4f_{5/2}$, $4f_{7/2}$) in (a) 1.0 and (b) 2.0Bi-LAS glasses and (c) Bi_2O_3 powders.

in bismuth-doped La_2O_3-Al_2O_3-SiO_2 glasses, given that the valence state of the target ion becomes higher with increasing bonding energy[24].

The NIR emissions of bismuth-doped La_2O_3-Al_2O_3-SiO_2 glasses is associated with two centers with low valence state species of Bi. The contributions of low valence state Bi, such as Bi^+ or Bi^0, to NIR emission have been reported in some bismuth-doped materials[8,10,16,23,24,26]. Following the hypothesis of Wu *et al.*[23] for NIR emissions in Bi-doped glass preforms and fibers, we ascribed the NIR emission of Bi-LAS glasses to both Bi^+ and Bi^0. The hypothesis is also supported by Wang's investigation on bismuth-doped phosphate glasses[26]. The schematic energy level diagrams for Bi^+[25] and Bi^0[16] are shown in Fig. 6. The absorption peaks identified in Fig. 1 are roughly matched to the proposed energy levels of Bi^0 and Bi^+. The emission at approximately 1 100 nm matches well with the transition from $(1)^2D_{3/2}$ to $^4S_{3/2}$ of Bi^0.

The emission band at approximately 1 300 nm can be attributed to the $^3P_1 \rightarrow {}^3P_0$ transition of Bi^+.

Figure 7 shows the decay curves of bismuth-doped La_2O_3-Al_2O_3-SiO_2 glasses in various doping levels excited at 500 nm. The inset plots the 1/e lifetime of each sample, detected at 1 150 nm, as a function of the Bi_2O_3 content. In Fig. 7, the lifetimes of the Bi-LAS samples decrease from 420 to 230 μs as the Bi_2O_3 content increases, indicating the occurrence of concentration quenching. The inset shows that the lifetime quickly decreases at low Bi_2O_3 contents (in 0.5, 1.0, and 2.0Bi-LAS). The lifetime then changes slightly as the Bi_2O_3 content increased. The decay curves and the 1/e lifetime of the 1 100-nm emission under 700-nm excitation follow a similar concentration dependence (Fig. 7).

The influence of temperature on NIR emissions and decay properties was investigated at series temperatures ranging from 9 to 350 K on a 2.0Bi-LAS glass sample with 1-mm thickness.

Figure 8 shows the temperature-dependent emission spectra (a) and the decay curves of the 1 170-nm emission (b) of the 2.0Bi-LAS sample excited at 500 nm. The inset of Fig. 8(b) plots the 1/e lifetime as a function of temperature. When the temperature increases from 9 to 350 K, the peak wavelengths and the FWHMs of emission bands remain constant at approximately 1 170 and 220 nm, respectively. Figures 8(a) and (b) show that the shapes of emission spectra and decay curves are approximately unchanged as the temperature varies. The inset of Fig. 8(b) shows that the lifetime of 2.0Bi-LAS is approximately 460 μs, and remains almost constant when the temperature increased from 9 to 350 K. The observation is similar to previous findings on Bi-doped LAS glass[23] and Bi-doped germanate glass[9]. The nearly-independent lifetime shows that the non-radiative decay process does not significantly occur until 350 K, and that NIR emissions have strong resistance to thermal quenching.

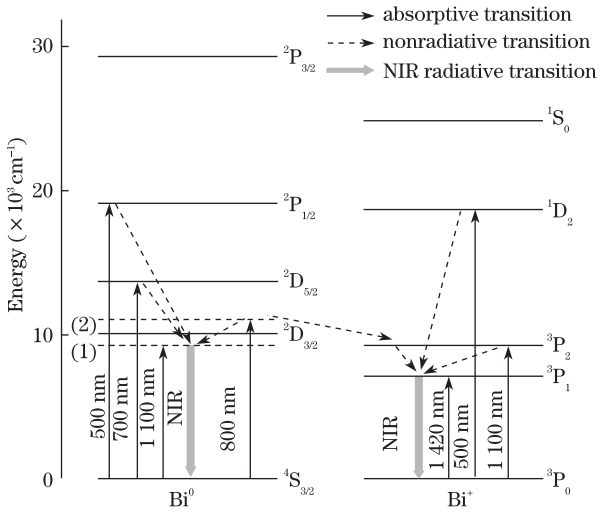

Fig. 6. Schematic energy level diagrams of Bi^0 and Bi^+ ions.

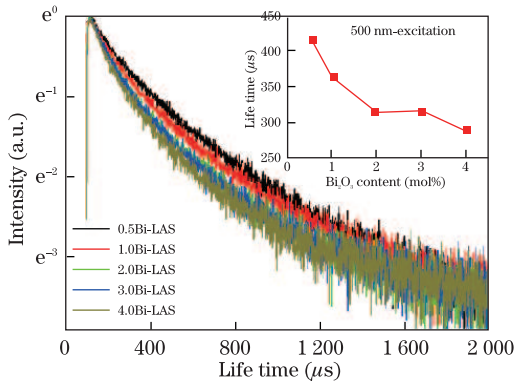

Fig. 7. Decay curves of Bi-LAS samples under 500-nm excitation. The inset shows lifetime as a function of Bi_2O_3 content.

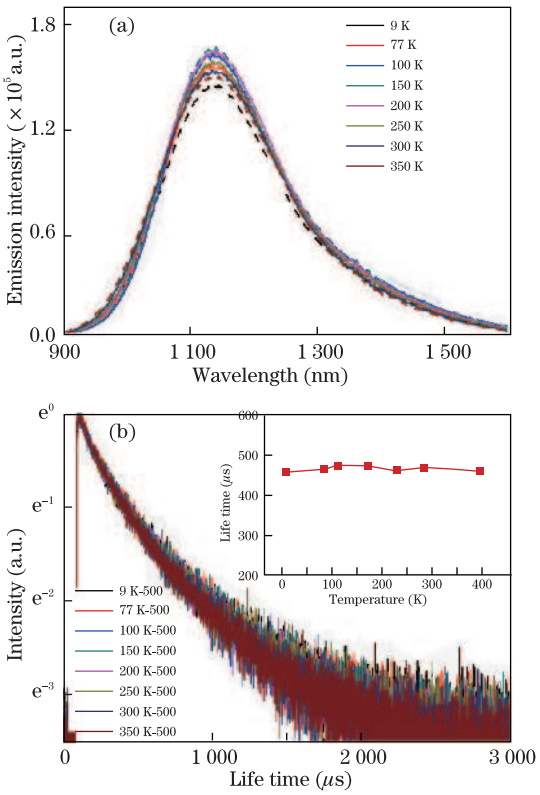

Fig. 8. (a) Emission spectra and (b) decay curves of the 1 170-nm emission of 2.0Bi-LAS under 500-nm excitation at different measuring temperatures. The inset of (b) shows the 1/e lifetime of 2.0Bi-LAS as function of temperature.

In conclusion, the impact of doping levels and temperature on the spectroscopic properties of Bi_2O_3-doped La_2O_3-Al_2O_3-SiO_2 glasses are investigated. The absorption cross section, σ_{abs}, increases as the Bi_2O_3 content increases. The absorption cross section reaches 8.31×10^{-21}cm^2 at the 500-nm excitation when the Bi_2O_3 content is 2.58 mol%. The emission intensity reaches a maximum value when the Bi_2O_3 content is 1.83 mol%. The emission peaks are at 1 190 and 1 117 nm, and the FWHM data are 330 and 228 nm at the 500 and 700-nm excitations, respectively. Two NIR emission centers, Bi^0 and Bi^+, are responsible for the NIR emission bands of Bi_2O_3-doped La_2O_3-Al_2O_3-SiO_2 glasses. The different concentration dependencies of emission centers are the most likely causes of the red shift and the broadening of emission bands as bismuth content increases. In addition, the fluorescent lifetime decreases from 420 to 230 μs as the Bi_2O_3 content increases from 0.40 % to 2.58% (in mol%).

Low temperature spectroscopic results show that the fluorescent lifetime of Bi-LAS glass is almost constant from 9 to 350 K. The nearly-independent lifetime suggests that the NIR emission of Bi in the system has strong resistance to thermal quenching.

The work was supported by the National Natural Science Foundation of China (Nos. 60937003 and 61111120100).

References

1. Y. Fujimoto and M. Nakatsuka, Jpn. J. Appl. Phys. **40,** 279 (2001).
2. Y. Fujimoto and M. Nakatsuka, Appl. Phys. Lett. **82,** 3325 (2003).
3. M. Peng, J. Qiu, D. Chen, X. Meng, and C. Zhu, Opt. Express **13,** 6892 (2005).
4. Z. Song, Z. Yang, D. Zhou, Z. Yin, C. Li, R. Wang, J. Shang, K. Lou, Y. Xu, X. Yu, and J. Qiu, J. Lumin. **131,** 2593 (2011).
5. M. A. Hughes, T. Suzuki, and Y. Ohishi, J. Non-Cryst. Solids **356,** 2302 (2010).
6. M. Peng, D. Chen, J. Qiu, X. Jiang, and C. Zhu, Opt. Mater. **29,** 556 (2007).
7. X. Meng, M. Peng, D. Chen, L. Yang, X. Jiang, C. Zhu, and J. Qiu, Chin. Phys. Lett. **22,** 615 (2005).
8. J. Ren, J. Qiu, D. Chen, X. Hu, X. Jiang, and C. Zhu, J. Alloy. Comp. **463,** L5 (2008).
9. T. Suzukia and Y. Ohishi, Appl. Phys. Lett. **88,** 191912 (2006).
10. X. Meng, J. Qiu, M. Peng, D. Chen, Q. Zhao, X. Jiang, and C. Zhu, Opt. Express **13,** 1628 (2005).
11. B. Denker, B. Galagan, V. Osiko, S. Sverchkov, and E. Dianov, Appl. Phys. B **87,** 135 (2007).
12. M. Peng, N. Zhang, L. Wondraczek, J. Qiu, Z. Yang, and Q. Zhang, Opt. Express **19,** 20799 (2011).
13. M. Peng, C. Wang, D. Chen, J. Qiu, X. Jiang, and C. Zhu, J. Non-Cryst. Solids **351,** 2388 (2005).
14. M. Hughes, T. Suzuki, and Y. Ohishi, J. Opt. Soc. Am. B **25,** 1380 (2008).
15. J. Ren, J. Qiu, D. Chen, X. Hu, X. Jiang, and C. Zhu, Solid State Commun. **141,** 559 (2007).
16. M. Peng, C. Zollfrank, and L. Wondraczek, J. Phys. Condens. Matter **21,** 285106 (2009).
17. M. Hughes, T. Akada, T. Suzuki, Y. Ohishi, and D. W. Hewak, Opt. Express **17,** 19345 (2009).
18. G. Dong, X. Xiao, J. Ren, J. Ruan, X. Liu, J. Qiu, C. Lin, H. Tao, and X. Zhao, Chin. Phys. Lett. **25,** 1891 (2008).
19. S. Iftekhar, J. Grins, and M. Edén, J. Non-Cryst. Solids **356,** 1043 (2010).
20. S. Iftekhar, E. Leonova, and M. Edén, J. Non-Cryst. Solids **355,** 2165 (2009).
21. V. V. Dvoyrin, V. M. Mashinsky, L. I. Bulatov, I. A. Bufetov, A. V. Shubin, M. A. Melkumov, E. F. Kustov, E. M. Dianov, A. A. Umnikov, V. F. Khopin, M. V. Yashkov, and A. N. Guryanov, Opt. Express **31,** 2966 (2006).
22. V. V. Dvoyrin, V. M. Mashinsky, and E. M. Dianov, IEEE J. Quantum Electron. **44,** 834 (2008).
23. J. Wu, D. Chen, X. Wu, and J. Qiu, Chin. Opt. Lett. **9,** 071601 (2011).
24. Y. Fujimoto, J. Am. Ceram. Soc. **93,** 581 (2010).
25. S. Zhou, N. Jiang, B. Zhu, H. Yang, S. Ye, G. Lakshminarayana, J. Hao, and J. Qiu, Adv. Funct. Mater. **18,** 1407 (2008).
26. X. Wang, Q. Sheng, L. Hu, and J. Zhang, Mater. Lett. **66,** 156 (2012).
27. Z. Yang, Z. Liu, Z. Song, D. Zhou, Z. Yin, K. Zhu, and J. Qiu, J. Alloy. Compd. **509,** 6816 (2011).